Dynamic interactions of Fc gamma receptor IIB with filamin-bound SHIP1 amplify filamentous actin-dependent negative regulation of Fc epsilon receptor I signaling.

Renaud Lesourne, Wolf H. Fridman, Marc Daëron

Dynamic interactions of FcγRIIB with filamin-bound SHIP1 amplify F-actin-dependent negative regulation of FcεRI signaling

Renaud Lesourne[*,†], Wolf H. Fridman[*] and Marc Daëron[*,†]

[*] Laboratoire d'Immunologie Cellulaire & Clinique, INSERM U. 255, Institut Biomédical des Cordeliers, 75006 Paris, France,

[†]Unité d'Allergologie Moléculaire & Cellulaire, Institut Pasteur, 75015 Paris, France.

Running title: Interactions of FcγRIIB with filamin-bound SHIP1

Keywords: Mast cells; Fc Receptors; Signal transduction

Abstract

The engagement of high-affinity receptors for IgE (FcεRI) generates both positive and negative signals whose integration determines the intensity of mast cell responses. FcεRI positive signals are also negatively regulated by low-affinity receptors for IgG (FcγRIIB). Although the constitutive negative regulation of FcεRI signaling was shown to depend on the sub-membranous F-actin skeleton, the role of this compartment in FcγRIIB-dependent inhibition is unknown. We show here that the F-actin skeleton is essential for FcγRIIB-dependent negative regulation. It contains SHIP1, the phosphatase responsible for inhibition, which is constitutively associated with the actin-binding protein, filamin-1. Following coaggregation, FcγRIIB and FcεRI rapidly interact with the F-actin skeleton and engage SHIP1 and filamin-1. Later on, filamin-1 and F-actin dissociate from FcR complexes while SHIP1 remains associated with FcγRIIB. Based on these results, we propose a dynamic model according to which the sub-membranous F-actin skeleton forms an inhibitory compartment where filamin-1 functions as a donor of SHIP1 for FcγRIIB which concentrate this phosphatase in the vicinity of FcεRI and thereby extinguish activation signals.

Introduction

Cell signaling takes place in specialized compartments. Based on their structural organization, biophysical properties and cellular localization, two main compartments were described. One consists of lipid rafts. These discrete membrane areas also known as low-density detergent-resistant membrane domains (LD-DRM), are composed of tightly packed glycosphingolipids and cholesterol organized in a liquid-ordered phase (1,2). Because signaling molecules are concentrated in lipid rafts while others are excluded, these have been proposed to function as signaling platforms. Another compartment consists of an F-actin cross-linked web, connected to the plasma membrane by a series of linkages between F-actin skeleton proteins and integral membrane proteins (sub-membranous F-actin skeleton) (3). Like lipid rafts, the sub-membranous F-actin skeleton is insoluble in nonionic detergents, but unlike rafts it is recovered in high-density fractions of sucrose gradients (4). This compartment plays a role in many cell functions involving morphological changes, such as phagocytosis, endocytosis, exocytosis, chemotaxis and cell division. It is also involved in cell signaling because F-actin can recruit, directly (5) or *via* actin-binding proteins (6), signaling molecules in sub-membranous areas where signaling complexes build up and function. Lipid rafts and sub-membranous F-actin skeleton dynamically interact with each other (7) and thus, act in concert to spatially organize cell signaling events.

Cells can receive numerous signals simultaneously, including positive and negative signals, that can be delivered by different membrane receptors, and whose integration determines cell responses. Receptors for the Fc portion of immunoglobulins (FcR) are such receptors. They comprise activating and inhibitory FcRs (8). Mast cells have been extensively used as a model to study FcR signaling. They express FcεRI, a prototypic activating receptor, and FcγRIIB, a prototypic inhibitory receptor. FcεRI are composed of an IgE-binding subunit (FcεRIα) and of two signaling subunits (FcRβ and FcRγ) which contain, each, an

Immunoreceptor Tyrosine-based Activation Motif (ITAM). Upon receptor aggregation, ITAMs are phosphorylated by the raft-associated src family tyrosine kinase Lyn (9,10). Phosphorylated ITAMs subsequently recruit SH2 domain-containing protein tyrosine kinases and adapters that initiate the constitution of signaling complexes where intracellular enzymes an substrates can meet and interact. One critical metabolite is phosphatidylinositol (3,4,5)-trisphosphate (PIP3) which mediates the recruitment of molecules that contain a plekstrin homology (PH) domain (11). Two consequences of these interactions are an increase in the concentration of intracellular Ca^{2+} and the activation of MAPKs that activate transcription factors. Altogether, these events lead to exocytosis and the subsequent release of granular mediators, to the production of newly formed lipid-derived inflammatory mediators, to the transcription of cytokine genes and the secretion of their products. FcγRIIB are single-chain receptors that bind IgG immune complexes with a high avidity. They contain one Immunoreceptor Tyrosine-based Inhibition Motif (ITIM) in their intracytoplasmic domain. Upon coaggregation with FcεRI by immune complexes, FcγRIIB inhibit mast cell activation (12). Coaggregation enables the FcεRI-associate kinase lyn to phosphorylate the ITIM of FcγRIIB (13). When phosphorylated, FcγRIIB recruit the SH2 domain-containing 5'-inositol phosphatase SHIP1 (14). SHIP1 was shown to be necessary and sufficient for FcγRIIB-dependent negative regulation (15). It interferes with positive signaling by two mechanisms. By dephosphorylating PIP3, it prevents the recruitment of molecules with a PH domain and the subsequent Ca^{2+} mobilization (16). By recruiting rasGAP *via* the adaptor molecule Dok-1, it down regulates the activation of MAPKs and the subsequent cytokine gene transcription (17).

Lipid rafts have been shown to play an essential role in organizing positive signaling by FcεRI. Disruption of rafts, using cholesterol-depleting drugs, dramatically decreases early phosphorylation events induced upon FcεRI aggregation (18). According to a current model,

FcεRI are excluded from rafts in resting mast cells, whereas signaling proteins covalently associated with saturated fatty acids, like Lyn (19) and LAT (20), are concentrated in these domains. Upon aggregation, FcεRI translocate into rafts (21) which coalesce (22), bringing in proximity FcεRI and raft-associated signaling proteins. Unlike rafts, the sub-membranous F-actin skeleton does not seem to be critical for FcεRI-dependent positive signaling. Observations suggest on the contrary, that the sub-membranous F-actin skeleton is involved in constitutive negative regulation of FcεRI signaling. Indeed, drugs such as latrunculin, which prevent actin polymerization, increase the rate and extent of antigen-induced degranulation (23). The inhibition of mast cell activation observed in excess of antigen is correlated with an association of FcεRI with actin microfilaments (24). SHIP1 was previously shown to constitutively down-regulate FcεRI signaling. Bone Marrow-derived Mast Cells (BMMCs) from SHIP1$^{-/-}$ mice indeed develop increased IgE-induced responses compared to BMMCs from wild-type littermates (25). Interestingly, SHIP1 and the related phosphatase SHIP2 were reported to associate with the sub-membranous F-actin skeleton upon thrombin activation in human platelets (26,27). In COS7 cells, the actin-binding protein filamin-1, was shown to mediate the constitutive association of SHIP2 with the sub-membranous F-actin skeleton (28).

Taken together, the above observations indicate that FcεRI signaling is controled by constitutive and by FcγRIIB-dependent negative regulation and that both depend on SHIP1. Constitutive negative regulation of FcεRI signaling was shown to depend on F-actin skeleton but the molecular basis of the recruitment of SHIP1 by FcεRI is unknown. Conversely, the molecular basis of the recruitment of SHIP1 by FcγRIIB is well established but the cellular basis of FcγRIIB-dependent negative regulation of FcεRI signaling is unknown. We investigated here the role of the sub-membranous F-actin skeleton in the inhibition of IgE-induced mast cell activation by FcγRIIB. We found that the F-actin skeleton is necessary for

FcγRIIB-dependent negative regulation of mast cell activation. Following coaggregation with FcεRI, FcγRIIB interact with the F-actin skeleton compartment, which contains the high-molecular weight isoform of SHIP1 that is constitutively associated with the actin-binding protein, filamin-1. Following coaggregation of receptors, SHIP1 and filamin-1 rapidly redistribute in small FcR patches. As FcR patches enlarge with time, filamin-1 and F-actin are excluded while SHIP1 remains colocalized with FcRs. Based on these results, we propose that, following the coaggregation of FcγRIIB with FcεRI, FcRs transiently interact with the F-actin skeleton, enabling FcγRIIB to recruit SHIP1 which is provided by filamin-1.

Materials and methods

Cells and transfectants. The rat mast cells RBL-2H3 were cultured in DMEM or RPMI supplemented with 10% FCS, 100 IU/ml penicillin, 100 µg/ml streptomycin and 2 mM L-glutamine. Culture reagents were from Gibco-BRL (Paisley, Scotland, UK). Clones of RBL-2H3 cells, stably transfected with cDNA encoding either murine FcγRIIB1 or a truncated form of murine FcγRIIB1 deleted for the nucleotide sequence (1059-1326) corresponding to the intracytoplasmic domain (FcγRIIB-IC$^-$), were described previously (29).

Antibodies and reagents. The mouse IgE mAb SPE-7 was purchased from Sigma (Saint-Louis, MO). The rat anti-mouse FcγRIIB mAb 2.4G2 was purified by affinity-chromatography on Protein G-sepharose from ascitic fluid of nude mice inoculated with 2.4G2 hybridoma cells intraperitoneally. F(ab')$_2$ fragments were obtained by pepsin digestion for 48h at 37°C. Fab' fragment were obtained by reduction of F(ab')$_2$ fragments with β-mercaptoethanol for 30 min at room temperature. The purity of IgG, F(ab')$_2$ and Fab' fragments was assessed by SDS-PAGE analysis. Their ability to recognize FcγRIIB was assessed by indirect immunofluorescence. Mouse anti-rat (MAR) F(ab')$_2$ were purchased from Jackson ImmunoResearch Laboratories (West Grove, PA). Rabbit antibodies against soluble recombinant extracellular domains of FcγRIIB were gifts from Pr. Catherine Sautès-Fridman (Institut Biomédical des Cordeliers, Paris, France). Mouse mAb against the FcRβ chain of FcεRI (JRK) were gifts from Dr. Jean-Pierre Kinet (Beth Israel Deaconess Medical Center and Harvard Medical School, Boston, MA). Mouse mAb against SHIP1 and filamin-1, rabbit antibodies against α-actinin, and goat antibodies against actin were purchased from Santa Cruz Biotechnology (Santa Cruz, CA), mouse mAb against cyclin D3 from New England Biolabs (Beverly, MA), mouse IgG2a used as isotype controls from Southern Biotechnologies (Birmingham, AL), HRP-labeled cholera toxin from Sigma, alexa 488-

labeled phalloidin from Molecular Probes (Eugene, OR) and HRP-conjugated Goat anti-Rabbit, Rabbit anti-Goat and Goat anti-Mouse immunoglobulins antibodies from Santa Cruz Biotechnology. Latrunculin B was purchased from Sigma.

Antibody labeling. IgE, 2.4G2 $F(ab')_2$ and Fab' fragments were iodinated by incubating antibodies with chloramine T and iodine-125 (^{125}I) (Amersham Bioscience, Piscataway, NJ) for 2 min at room temperature. The reaction was stopped by natriumdisulfide and kaliumiodide. MAR $F(ab')_2$ were trinitrophenylated by incubation for 2 h at room temperature with trinitrobenzene sulfonic acid (Eastman Kodak, Rochester, NY) in borate-buffered saline pH 8.0. Iodinated antibodies and TNP_{13-18}-MAR $F(ab')_2$ were purified on Sephadex G25 (Pharmacia Fine Chemicals, Uppsala, Sweden). For confocal microscopy analysis, all antibodies were labeled and purified using the Amersham CyDye Fluoro link labelling kits.

Cell stimulation. In radioactivity experiments 2-3x10^7 cells at 5x10^6 cells/ml were incubated with 0.5 µg/ml unlabeled and ^{125}I-labeled IgE anti-DNP and/or with 1 µg/ml unlabeled or 0.1 ^{125}I-labeled 2.4G2 $F(ab')_2$ for 1 h at 37°C. Cells were washed, resuspended at 1x10^7 cells/ml and stimulated with TNP-MAR $F(ab')_2$. MAR $F(ab')_2$ were moderately substituted with TNP to ensure that they could bind efficiently 2.4G2. For the biochemical analysis of SHIP1 recruitment by FcγRIIB, 5x10^7 cells were stimulated as described above. For confocal microscopy experiments, 1.5x10^6 cells were incubated with 3 µg/ml Cy3-IgE anti-DNP and 1 µg/ml Cy5-2.4G2 $F(ab')_2$ for 1 h at 37°C. Cells were stimulated with 30 µg/ml TNP_{13}-MAR $F(ab')_2$ for 4 min or the indicated periods of time.

Subcellular fractionation. *Cytosol, Membrane and F-actin skeleton fractionation:* All procedures were performed at 0-4°C. 3x10^7 cells (for radioactivity experiments) or 8-9x10^7

cells (for Western blot analysis) were incubated at $6x10^7$ cells/ml for 15 min with hypotonic lysis buffer (25 mM Hepes pH 6.9, 10 mM KCl, 10 µg/ml aprotinin and 1 mM PMSF), and disrupted with a tight-fitting pestle (VWR, West Chester, PA). Cell lysates were centrifuged for 3 min at 1,000g, supernatants were recovered and centrifuged at 15,000g for 30 min. Supernatants (cytosolic fraction) were collected, and pellets were resuspended and incubated for 15 min in Triton X-100 (TX-100) lysis buffer (10 mM Tris pH 7.4, 50 mM NaCl, 1% TX-100, 1 mM Na_3VO_4, 5 mM NaF, 5 mM sodium pyrophosphate, 0.4 mM EDTA, 10 µg/ml aprotinin, 10 µg/ml leupeptin and 1 mM PMSF). Cell lysates were centrifuged at 15,000 g for 30 min. Supernatants (membrane fraction) were collected and pellets (F-actin skeleton fraction) were resuspended in SDS/octylglucoside/TX-100 lysis buffer (10 mM Tris pH 7.4, 50 mM NaCl, 1% TX-100, 10 mM n-Ocytl-β-D-glucopyranoside, 0.5% SDS, 1 mM Na_3VO_4, 5 mM NaF, 5 mM sodium pyrophosphate, 0.4 mM EDTA, 10 µg/ml aprotinin, 10 µg/ml leupeptin and 1 mM PMSF). In radioactivity experiments, fractions were counted with a γ counter and the percentages of radioactivity were calculated as indicated in figures. For Western blot analysis, proteins were quantified in each fraction with the Dc protein assay from Biorad (Hercules, Ca). 100 µg of proteins were electrophoresed in SDS polyacrylamide gel. *Preparation of Low-Density Detergent-Resistant Membrane domains (LD-DRM)*: All procedures were performed at 0-4°C. $2x10^7$ cells were incubated with 1 ml TX-100_{low} lysis buffer (25 mM Hepes pH 7.4, 50 mM NaCl, 0.1% or 0.06 % Triton X-100, 1 mM Na_3VO_4, 5 mM NaF, 5 mM sodium pyrophosphate, 0.4 mM EDTA, 10 µg/ml aprotinin, 10 µg/ml leupeptin and 1 mM PMSF) for 30 min. Lysates were mixed in polyallomer centrifuge tubes (Beckman, Fullerton, Ca) with an equal volume of 85 % sucrose in a solution of 25 mM Hepes pH 7.4, 150 mM NaCl. Mixtures were successively overlaid with 6 ml 30 % sucrose and 3 ml 5 % sucrose. Tubes were centrifuged at 200,000 g in a Beckman SW41 Ti rotor for 16 h. One-ml fractions were harvested from the top of the gradient and counted with a γ

counter. For Western blot analysis, 100 µl 100 mM n-Ocytl-β-D-glucopyranoside and 5% SDS were added in fractions before loading equal volumes on an SDS polyacrylamide gel.

Immunoprecipitation and Western blot analysis. Cells were lysed at 0°C for 15 min in TX-100 lysis buffer and further disrupted with a tight-fitting pestle. Cell lysates were centrifuged at 12,000 g and post-nuclear supernatants were collected. For FcγRIIB immunoprecipitation, Protein G-sepharose beads (Pharmacia) were used to precipitate 2.4G2-bound FcγRIIB. For filamin-1 immunoprecipitation, Protein G-sepharose beads were coated with anti-filamin-1 antibodies for 2 h at room temperature. Adsorbents were incubated with post-nuclear lysates for 2 h at 4°C, washed in lysis buffer and boiled for 3 min in sample buffer. Eluted material was fractionated by SDS-PAGE and transferred onto Immobilon-P membranes (Millipore, Bedford, MA, USA). Membranes were saturated with either 5% BSA (Sigma) or 5% skimmed milk (Régilait, Saint-Martin-Belle-Roche, France) diluted in 10mM Tris buffer pH 7.4 containing 0.5% Tween 20 (VWR), and Western blotted with the indicated antibodies followed by HRP-conjugated Goat anti-Rabbit, Rabbit anti-Goat, or Goat anti-Mouse immunoglobulins antibodies. Labeled antibodies were detected using the Amersham ECL kit.

Indirect immunofluorescence. Cells were incubated with medium alone, 0.5 µg/ml IgE anti-DNP or 2 µg/ml 2.4G2 $F(ab')_2$ with or without 0.25 µg/ml latrunculin B for 18 h at 37°C. Cells were harvested, fixed with 3% paraformaldehyde (PFA) and stained for 1 h at room temperature with alexa 488-phalloidin, FITC-GAM $F(ab')_2$ (to reveal IgE) or FITC-MAR $F(ab')_2$ (to reveal 2.4G2). Fluorescence was analyzed by flow cytometry using a FACScalibur (Becton Dickinson, Mountain View, CA).

Confocal Microscopy. After stimulation, cells were centrifuged and incubated for 20 min at room temperature in 3% PFA. Cells were washed with PBS and permeabilized with 0.05% saponin in PBS supplemented with 0.2% BSA. Permeabilized cells were stained for 1 h at room temperature with FluorX- or Cy5-anti-SHIP1 antibodies, FluorX-anti-filamin-1 antibodies, or alexa 488-phalloidin. Cells were washed in PBS, resuspended in mowiol medium (VWR) and mounted between a Superfrost slide and a mico cover glass (VWR). Confocal laser scanning microscopy was performed using a Zeiss LSM510 microscope (Carl Zeiss, Oberkochen, Bade-Wurtemberg, Germany). Simultaneous double or triple fluorescence acquisitions were performed using the 488-, 543- and 633-nm laser lines and a 63x oil immersion Plan-Apochromat objective (NA = 1.4). The depth of field was of 1 µm. FcR patches in which IgE-Cy3 and Cy5-2.4G2 F(ab')$_2$ colocalized were mesured using the Zeiss AIM 2.5 software.

β-hexosaminidase release. Cells were sensitized with 0.1 µg/ml IgE anti-DNP with or without 2 µg/ml 2.4G2 F(ab')$_2$ for 18 h at 37°C. When indicated, 0.25 µg/ml latrunculine B was added in cultures. Cells were washed, pre-warmed for 15 min at 37°C with or without 0.25 µg/ml latrunculin B, and stimulated with 10 µg/ml TNP_{13}-MAR F(ab')$_2$ for 30 min at 37°C. Reactions were stopped on ice and supernatants were collected. β-hexosaminidase release was measured by incubating supernatants with *p*-nitrophenyl-*N*-acetyl-D-glucosaminide (a β-hexosaminidase substrate) (Sigma) for 2 h at 37°C. Reactions were stopped with glycine 0.2 M pH 10.7, and absorbance was measured at 405 nm. The percentages of β-hexosaminidase released in supernatants were calculated using as 100 % β-hexosaminidase contained in aliquots of cells lysed in 1 % TX-100.

Results

1. F-actin skeleton disruption decreases FcγRIIB-dependent inhibition of IgE-induced mediator release by mast cells.

To investigate the role of the F-actin skeleton in FcγRIIB-dependent negative regulation of IgE-induced mast cell activation, we examined FcγRIIB-dependent inhibition in cells treated with a drug that prevents F-actin polymerization. Cells were incubated with latrunculin B under conditions that had no effect on mediator release observed following FcεRI aggregation. This treatment reduced the amount of F-actin but not the expression of FcγRIIB and FcεRI (Fig. 1A). FcγRIIB-dependent inhibition of β-hexosaminidase release observed in untreated cells was decreased in latrunculin-treated cells (Fig. 1B). An intact F-actin skeleton is therefore required for optimal inhibition of mast cell activation by FcγRIIB.

2. When coaggregated or aggregated, FcγRIIB and FcεRI translocate into the F-actin skeleton compartment.

To investigate whether FcγRIIB can interact with the F-actin skeleton upon coaggregation with FcεRI, cytosol, membrane and F-actin skeleton fractions were prepared and analyzed by Western blotting. In unstimulated cells, the F-actin-associated protein α-actinin was recovered in the F-actin skeleton fraction, but also in the cytosol fraction. Cyclin D3 was found in the cytosol fraction only. FcγRIIB were recovered in the membrane fraction only (Fig. 2A).

When quantitated with ^{125}I-labeled 2.4G2 F(ab')$_2$ in resting cells, most FcγRIIB were also recovered in the membrane fraction (75%), but some were recovered in the cytosol fraction (15%) and in the F-actin skeleton fraction (10%). Following coaggregation with FcεRI, two-fold less FcγRIIB were recovered in the membrane fraction while five-fold more

were recovered in the F-actin skeleton fraction, reaching 50% of total FcγRIIB (Fig. 2B). The same was observed following FcγRIIB aggregation, indicating that FcγRIIB do not need to be coaggregated with FcεRI to translocate into the F-actin skeleton compartment (Fig. 2C). Noticeably, upon aggregation, FcγRIIB with a deletion of their whole intracytoplasmic domain (FcγRIIB-IC$^-$), redistributed in the F-actin skeleton fraction in the same proportion as intact FcγRIIB (Fig. 2C).

Likewise, when quantitated using ^{125}I-IgE, the proportion of FcεRI recovered in the F-actin skeleton fraction increased upon aggregation. This increase varied in parallel with the concentration of ligand. The proportion of FcεRI recovered in the F-actin skeleton fraction following aggregation was however lower than the proportion of FcγRIIB recovered in this fraction upon aggregation. When coaggregated with FcγRIIB, the proportion of FcεRI that translocated into the F-actin skeleton compartment increased to similar values. It however reached a plateau at a lower concentration of ligand. This result indicates that coaggregation with FcγRIIB facilitates the translocation of FcεRI into the F-actin skeleton compartment (Fig. 2D).

3. Following coaggregation with FcεRI, FcγRIIB remain excluded from LD-DRM.

Several raft markers like LAT, *lyn* and GM1, were recovered not only in the membrane fraction, but also in the F-actin skeleton fraction (data not shown). This observation raised the possibility that FcγRIIB interacted with lipid rafts, rather than with the F-actin skeleton. To discriminate between these two possibilities, cells were lysed in TX-100 and cell lysates were fractionated by ultracentrifugation in discontinuous sucrose gradients. Western blot analysis shows that, in unstimulated cells, the raft marker GM1 was recovered in fractions 3-4 containing LD-DRM (the interface between the low- and the middle-density solutions), whereas the F-actin skeleton marker α-actinin was recovered in fractions 10-11 (the high-

density solution). FcγRIIB had the same distribution as FcεRI. The vast majority of receptors were recovered in fractions 8-11. Minute amounts of receptors were recovered in fractions 3-4. SHIP1, the effector phosphatase of FcγRIIB-dependent inhibition, was detected in fractions 10-11 (Fig. 3A). To quantitate FcγRIIB in density fractions following coaggregation with FcεRI, cells were incubated with ^{125}I-labeled 2.4G2 F(ab')$_2$. They were sensitized with mouse IgE anti-DNP, challenged with TNP$_{18}$-MAR F(ab')$_2$ or not, and lysed in TX-100 (two concentrations were used). Lysates were fractionated as above. In unstimulated cells, FcγRIIB had the same distribution when assessed by radioactivity as when assessed by Western blotting. Following coaggregation with FcεRI, the amount of FcγRIIB recovered in LD-DRM did not increase, but rather decreased. Under these conditions, 75% FcγRIIB were recovered in fraction 11, at the bottom of the gradient (Fig. 3B, right panel). To check that we were able to detect receptor translocation into LD-DRM, we analyzed the translocation of FcεRI after receptor aggregation. Cells were incubated with ^{125}I-labeled mouse IgE anti-DNP and stimulated with TNP$_{18}$-MAR F(ab')$_2$. As previously described, the amount of FcεRI recovered in LD-DRM fractions increased following receptor aggregation. The absolute amounts of FcεRI recovered in these fractions depended on the concentration of detergent, but not the relative amounts (Fig. 3C).

Altogether, these results indicate that, when coaggregated with FcεRI, FcγRIIB translocate into material recovered at the bottom of the highest density fraction containing F-actin skeleton markers, but not detectably into LD-DRM.

4. The F-actin skeleton compartment contains the high-molecular weight isoform of SHIP1 that interacts with the actin-binding protein filamin-1 in resting cells.

SHIP2 was reported to associate constitutively with the F-actin skeleton in COS7 cells, and this association was found to be mediated by the actin-binding protein, filamin-1.

We investigated whether these findings could apply to SHIP1 in mast cells. Subcellular fractionation analysis of resting mast cells revealed that, although most SHIP1 was recovered in the cytosol fraction, SHIP1 was also recovered in the F-actin skeleton fraction. SHIP1 was hardly detectable in the membrane fraction. Noticeably, the two main isoforms of SHIP1 were found in comparable amounts in the cytosol fraction whereas the high-molecular weight isoform was predominant in the F-actin skeleton fraction (Fig 4A). Because SHIP2 was reported to constitutively associate with the F-actin skeleton *via* the actin-binding protein filamin-1 in COS7 cells (28), we compared the cellular localization of filamin-1 and SHIP1 in resting cells and we investigated whether these two proteins can interact. Filamin-1 was recovered with SHIP1 both in the cytosol and in the F-actin skeleton fraction (Fig. 4A). SHIP1 was colocalized with filamin-1, both in the cytosol and in cortical areas, when examined by confocal microscopy (Fig. 4B). SHIP1 coprecipitated with filamin-1 in resting cells (Fig. 4C). Noticeably, the high-molecular weight isoform of SHIP1 preferentially coprecipitated with filamin-1, whereas the low-molecular weight isoform was predominant in whole cell lysate (Fig. 4D). These results altogether indicate that the F-actin skeleton contains the high-molecular weight isoform of SHIP1 that is constitutively associated with the actin-binding protein filamin-1.

5. FcγRIIB and SHIP1 interact with filamin-1 upon coaggregation with FcεRI.

Interestingly, the high-molecular weight isoform of SHIP1 preferentially coprecipitated also with FcγRIIB following coaggregation with FcεRI (Fig. 4D). Since FcγRIIB translocate into the F-actin skeleton compartment and since the high-molecular weight isoform of SHIP1 is constitutively associated with filamin-1, we investigated whether FcγRIIB associate with filamin-1 upon coaggregation with FcεRI. We failed to detect any coprecipitation between FcγRIIB and filamin-1 (data not shown). We therefore examined

whether SHIP1, F-actin and filamin-1 colocalize with FcR patches formed upon coaggregation of FcεRI with FcγRIIB. Cells were incubated with Cy3-IgE and Cy5-2.4G2 $F(ab')_2$ prior stimulation with TNP-MAR $F(ab')_2$, and the colocalization of FcRs with SHIP1, filamin-1 and F-actin was examined separately. Following FcγRIIB coaggregation with FcεRI, SHIP1 and filamin-1, but not F-actin, were inducibly redistributed with FcR in small patches. Phalloidin staining was observed in cortical areas exclusively as in unstimulated cells and it remained superimposed with FcR clusters (Fig. 5A). The colocalization of SHIP1 with filamin-1 was also examined in individual cells. Following coaggregation of FcγRIIB with FcεRI, SHIP1 and filamin-1 accumulated and colocalized in small aggregates located in cortical areas (Fig. 5B). These results indicate that the coaggregation of FcγRIIB with FcεRI induces the redistribution of both SHIP1 and filamin-1 in small aggregates that colocalize with FcR patches.

6. SHIP1 remains in FcR patches while filamin-1 and F-actin are excluded, as patches enlarge with time.

In the majority of cells, FcR patches had a small size but large FcR patches were also seen. Noticeably, the percentage of cells with patches larger than 2 μm increased with time (Fig. 6A), suggesting that FcR patches progressively enlarge during the minutes following FcεRI/FcγRIIB coaggregation. SHIP1 remained clustered with FcγRIIB and FcεRI in large patches whereas, surprisingly, both filamin-1 and F-actin were excluded (Fig 6B). When examined in individual cells, filamin-1 was not colocalized with large SHIP1 aggregates (Fig. 6C). Quantitative analysis of filamin-1 and SHIP1 redistribution as a function of the size of FcR patches revealed that FcR patches containing filamin-1 had an average size of 1.4 ± 0.9 μm, whereas FcR patches not containing filamin-1 had an average size of 3.7 ± 0.9 μm. SHIP1 was observed in FcR patches whatever their size (0.8 to 5 μm) (Fig. 6D).

Altogether, these results show that, upon coaggregation of FcγRIIB with FcεRI, small clusters containing FcγRIIB, FcεRI, SHIP1, filamin-1 and F-actin form first, from which filamin-1 and F-actin are excluded as clusters enlarge with time at the cell surface.

Discussion

We show here that the F-actin skeleton is necessary for FcγRIIB-dependent negative regulation of IgE-induced mast cell activation and contains the effector molecule of inhibition, SHIP1, which is constitutively associated with the actin-binding protein filamin-1. The coaggregation of FcγRIIB with FcεRI induces the translocation of both FcRs in the F-actin skeleton compartment and the rapid redistribution of SHIP1 and filamin-1 with FcR membrane patches. Later on, filamin-1 and F-actin dissociate while SHIP1 remains associated with FcR aggregates. Based on these results, we propose a dynamic model according to which the F-actin skeleton functions as an inhibitory compartment and we suggest that the same inhibitory process operates in constitutive and FcγRIIB-dependent negative regulation of FcεRI signaling.

First of all, latrunculin-induced F-actin disruption was found to decrease FcγRIIB-dependent inhibition of mast cells' secretory response. It was previously reported that the treatment of RBL-2H3 cells with F-actin-disrupting drugs dramatically affects the cytosolic F-actin network but only marginally the sub-membranous F-actin skeleton (30). This result suggests that the decrease of FcγRIIB-dependent inhibition of mast cell degranulation induced by latrunculin primarily results from an alteration of the cytosolic F-actin network. This compartment therefore appears as an essential compartment not only for constitutive negative regulation of FcεRI signaling, but also for FcγRIIB-dependent negative regulation.

We found that SHIP1, which is required for both regulatory processes, is associated with the F-actin skeleton in resting cells. SHIP1 was indeed present in the cytosol, as expected, but also in the F-actin skeleton as revealed by biochemical analysis of subcellular fractions. SHIP1 was also colocalized with the actin-binding protein filamin-1, both in the cytosol and, together with F-actin, in cortical areas as shown by confocal microscopy. Finally,

SHIP1 coprecipitated with filamin-1 in whole cell lysates (Fig. 3B) and in cytosolic subcellular fractions (data not shown). These data suggest that a fraction of SHIP1 is associated with the sub-membranous F-actin *via* filamin-1. We however failed to coprecipitate SHIP1 with filamin-1 in the F-actin skeleton fraction. Very low amounts of soluble proteins were, indeed, recovered in this fraction, and the amount of immunoprecipitated filamin-1 may be too low for the coprecipitation of SHIP1 to be detectable. We noticed however that, although comparable amounts of the high- and low-molecular weight isoforms of SHIP1 (145 kDa and 135 kDa) are present in the cytosol, the high-molecular weight isoform preferentially interacts with the F-actin skeleton and with filamin-1. The two SHIP1 isoforms differ by a C-terminal sequence containing several polyproline motifs. This sequence, that is deleted in the 135-kDa isoform, may mediate the interaction of SHIP1 with filamin-1 and, consequently, with the F-actin skeleton. Supporting this contention, the C-terminal end of SHIP1 was proposed to be essential for the sub-membranous localization of the phosphatase (31). Moreover, the association of SHIP2 with filamin-1 depends on the proline-rich C-terminal end of this phosphatase (28). The sub-membranous F-actin skeleton appears therefore as a SHIP1-containing compartment where the 145-kDa isoform of SHIP1 is concentrated *via* filamin-1. This sub-membranous concentration of SHIP1 could provide an accessible pool of phosphatase for negative regulation of FcεRI signaling.

In resting cells, FcγRIIB was not found in the F-actin skeleton subcellular fraction. The vast majority of FcγRIIB was located in the membrane fraction. When coaggregated or aggregated independently, FcγRIIB and FcεRI translocated into the F-actin skeleton compartment. As observed by confocal microscopy, FcγRIIB and FcεRI accumulated in small membrane patches when coaggregated. F-actin did not accumulate in these patches but phalloidin staining remained however superimposed with FcR clusters. Following

aggregation, FcγRIIB and FcεRI may therefore become anchored to the F-actin network lying underneath FcR aggregates. Surprisingly, FcγRIIB translocation was not prevented when the intracytoplasmic domain of the receptors was deleted. An association of FcγRIIB with an F-actin-linked membrane protein may explain this observation. Supporting this hypothesis, it was reported that other low-affinity Fc receptors for IgG, FcγRIIA, can physically interact with the F-actin-associated αMβ2 integrin (32).

When coaggregated with FcεRI, FcγRIIB did not detectably translocate into LD-DRM-containing fractions. Moreover, the coaggregation of FcεRI with FcγRIIB partially inhibited FcεRI translocation into LD-DRM (data not shown). We reported previously that FcγRIIB are phosphorylated by the raft-associated tyrosine kinase Lyn upon coaggregation with FcεRI (13). This suggests that FcγRIIB require, somehow, to translocate into rafts in order to be phosphorylated. Kono *et al*. reported that FcγRIIB can translocate into LD-DRM upon aggregation in RBL-2H3 cells (33). A possible explanation is that FcγRIIB interact with rafts, but more weakly or more transiently than FcεRI. By contrast, FcγRIIB heavily translocated into material recovered at the bottom of sucrose gradients where F-actin skeleton markers are found. Our results therefore indicate that, following coaggregation with FcεRI, FcγRIIB translocate into the F-actin skeleton compartment rather than into lipid rafts.

When FcεRI and FcγRIIB were coaggregated, filamin-1 redistributed with FcRs and with SHIP1 in small membrane patches. These results support the hypothesis that, once associated with F-actin, FcγRIIB recruit filamin-bound SHIP1. Noticeably, we did not detect any substantial translocation of SHIP1 from the cytosol to membrane areas by confocal microscopy analysis (Fig. 5A). Likewise, fractionation analysis did not reveal any translocation of SHIP1 from the cytosol to membrane or F-actin skeleton (data not shown). As SHIP1 was hardly detected in the membrane fraction, these observations indicate that FcγRIIB anchoring to F-actin may bring and stabilize FcγRIIB close to SHIP1, enabling

receptors to recruit this phosphatase. Supporting this hypothesis, the 145-kDa isoform of SHIP1 that is preferentially associated with the F-actin skeleton and with filamin-1 preferentially coprecipitated with FcγRIIB.

An analysis of the dynamics of FcR patches revealed that the proportion of patches larger than 2 μm in size increased with time. Small patches may therefore coalesce to form larger patches. The raft marker GM1 (data not shown) and SHIP1 were present both in small and large patches. Filamin-1 and F-actin were present in small patches but excluded from large patches. SHIP1 remained therefore associated with FcRs but dissociated from filamin-1 as patches enlarged. FcRs may thus transiently interact with F-actin and filamin-1 upon coaggregation, which would explain why we failed to coprecipitate FcγRIIB with filamin-1, or filamin-1 with FcγRIIB (data not shown). Filamin-1 therefore appears as a donor of SHIP-1 for FcγRIIB. The exclusion of F-actin from large patches may result from a local depolymerization of actin microfilaments. FcγRIIB was reported to prevent F-actin polymerization in B cells upon coaggregation with BCR (34). As the length of actin filaments depends on the balance between polymerization and depolymerization that occur simultaneously, inhibition of polymerization may shorten actin filaments, thereby breaking down the sub-membranous F-actin network which filamin-1 is anchored to. These spatio-temporal redistributions of receptors, effectors, lipid rafts and F-actin skeleton are reminiscent of the supra-molecular activation cluster termed immunological synapse that forms between T cells and Antigen-Presenting Cells (35). Although induced by soluble ligands, synapse-like structures may thus build-up upon FcR engagement in mast cells, that would provide a dynamic "signalosome" enabling FcRs to be sequentially translocated in distinct compartments with antagonistic properties, and FcR signals to be sequentially turned on and turned off. The constitutive negative regulation of FcεRI signaling, especially when in excess of antigen, may result from the relocation of FcεRI-dependent activation signals close to

SHIP1 in the F-actin skeleton. If FcεRI signaling is constitutively down regulated by SHIP1, one can wonder what the contribution of FcγRIIB is in the inhibition of FcεRI signaling. The recruitment of SHIP1 by FcγRIIB was indeed reported to have no effect on the catalytic activity of SHIP1 (36). We propose that FcγRIIB negatively regulate FcεRI signaling by two mechanisms. First, they facilitate the translocation of FcεRI into the F-actin skeleton compartment, thus enhancing SHIP1-dependent constitutive negative regulation of FcεRI. This mainly occurs at low antigen concentrations. Second, FcγRIIB concentrate SHIP1 in the vicinity of FcεRI. Supporting this interpretation, SHIP1 readily coprecipitates with phopshorylated FcγRIIB but not with with FcεRI. Both the coprecipitation of SHIP1 and inhibition of mast cell activation (13), but not the translocation of FcγRIIB into the F-actin skeleton, require the intracytoplasmic domain of FcγRIIB. It follows that FcγRIIB act as amplifiers of SHIP1-dependent constitutive negative regulation of FcεRI signaling.

Acknowledgements:

We are grateful to Dr. Jean-Pierre Kolb and Dr. Jeanne Wietzerbin for having kindly hosted us in their laboratory at the Institut Curie to perform radioactivity experiments. We thank Dr. Christophe Klein for his help for confocal microscopy experiments. These were performed using the IFR 58 facilities at the Institut Biomédical des Cordeliers.

References

1. Brown, D. A., and E. London. 2000. Structure and Function of Sphingolipid- and Cholesterol-rich Membrane Rafts. *J. Biol. Chem. 275:17221.*
2. Horejsi, V. 2003. The roles of membrane microdomains (rafts) in T cell activation. *Immunol Rev 191:148.*
3. Luna, E. J., and A. L. Hitt. 1992. Cytoskeleton--plasma membrane interactions. *Science 258:955.*
4. Brown, D. A., and J. K. Rose. 1992. Sorting of GPI-anchored proteins to glycolipid-enriched membrane subdomains during transport to the apical cell surface. *Cell 68:533.*
5. Yao, L., P. Janmey, L. G. Frigeri, W. Han, J. Fujita, Y. Kawakami, J. R. Apgar, and T. Kawakami. 1999. Pleckstrin homology domains interact with filamentous actin. *J Biol Chem 274:19752.*
6. Stossel, T. P., J. Condeelis, L. Cooley, J. H. Hartwig, A. Noegel, M. Schleicher, and S. S. Shapiro. 2001. Filamins as integrators of cell mechanics and signalling. *Nat Rev Mol Cell Biol 2:138.*
7. Kwik, J., S. Boyle, D. Fooksman, L. Margolis, M. P. Sheetz, and M. Edidin. 2003. Membrane cholesterol, lateral mobility, and the phosphatidylinositol 4,5-bisphosphate-dependent organization of cell actin. *Proc Natl Acad Sci U S A 100:13964.*
8. Daëron, M. 1997. Fc Receptor Biology. *Annu. Rev. Immunol. 15:203.*
9. Pribluda, V. S., C. Pribluda, and H. Metzger. 1994. Transphosphorylation as the mechanism by which the high affinity receptor for IgE is phosphorylated upon aggregation. *Prc. Nat. Acad. Sci. USA 91:11246.*

10. Yamashita, T., S.-Y. Mao, and H. Metzger. 1994. Aggregation of the high-affinity IgE receptor and enhanced activity of p53/56lyn protein-tyrosine kinase. *Proc. Natl. Acad. Sci. USA 91:11251.*

11. Kawakami, Y., L. Yao, T. Miura, S. Tsukada, O. N. Witte, and T. Kawakami. 1994. Tyrosine phosphorylation and activation of Bruton tyrosine kinase upon FcεRI crosslinking. *Mol. Cell. Biol. 14:5108.*

12. Daëron, M., O. Malbec, S. Latour, M. Arock, and W. H. Fridman. 1995. Regulation of high-affinity IgE receptor-mediated mast cell activation by murine low-affinity IgG receptors. *J. Clin. Invest. 95:577.*

13. Malbec, O., D. Fong, M. Turner, V. L. J. Tybulewicz, J. Cambier, C., W. H. Fridman, and M. Daëron. 1998. FcεRI-associated lyn-dependent phosphorylation of FcγRIIB during negative regulation of mast cell activation. *J. Immunol. 160:1647.*

14. Ono, M., S. Bolland, P. Tempst, and J. V. Ravetch. 1996. Role of the inositol phosphatase SHIP in negative regulation of the immune system by the receptor FcγRIIB. *Nature 383:263.*

15. Ono, M., H. Okada, S. Bolland, S. Yanagi, T. Kurosaki, and J. V. Ravetch. 1997. Deletion of SHIP or SHP-1 reveals two distinct pathways for inhibitory signaling. *Cell 90:293.*

16. Bolland, S., R. N. Pearse, T. Kurosaki, and J. V. Ravetch. 1998. SHIP modulates immune receptor responses by regulating membrane association of Btk. *Immunity 8:509.*

17. Tamir, I., J. C. Stolpa, C. D. Helgason, K. Nakamura, P. Bruhns, M. Daëron, and J. C. Cambier. 2000. The RasGAP-binding protein p62dok is a Mediator of Inhibitory FcγRIIB Signals in B cells. *Immunity 12:347.*

18. Sheets, E. D., D. Holowka, and B. Baird. 1999. Critical role for cholesterol in Lyn-mediated tyrosine phosphorylation of FcεRI and their association with detergent-resistant membranes. *J Cell Biol 145:877.*

19. Young, R. M., D. Holowka, and B. Baird. 2003. A lipid raft environment enhances Lyn kinase activity by protecting the active site tyrosine from dephosphorylation. *J Biol Chem 278:20746.*

20. Zhang, W., R. P. Trible, and L. E. Samelson. 1998. LAT palmitoylation: its essential role in membrane microdomain targeting and tyrosine phosphorylation during T cell activation. *Immunity 9:239.*

21. Field, K. A., D. Holowka, and B. Baird. 1997. Compartmentalized activation of the high affinity immunoglobulin E receptor within membrane domains. *J Biol Chem 272:4276.*

22. Thomas, J. L., D. Holowka, B. Baird, and W. W. Webb. 1994. Large-scale co-aggregation of fluorescent lipid probes with cell surface proteins. *J Cell Biol 125:795.*

23. Frigeri, L., and J. R. Apgar. 1999. The role of actin microfilaments in the down-regulation of the degranulation response in RBL-2H3 mast cells. *J Immunol 162:2243.*

24. Seagrave, J., and J. M. Oliver. 1990. Antigen-dependent transition of IgE to a detergent-insoluble form is associated with reduced IgE receptor-dependent secretion from RBL-2H3 mast cells. *J Cell Physiol 144:128.*

25. Huber, M., C. D. Helgason, J. E. Damen, L. Liu, R. K. Humphries, and G. Krystal. 1998. The src homology 2-containing inositol phosphatase (SHIP) is the gatekeeper of mast cell degranulation. *Proc. Natl. Acad. Sci. USA 95:11330.*

26. Giurato, s., B. Payrastre, A. L. Drayer, M. Plantavid, R. Woscholski, P. Parker, and C. Erneux. 1997. Tyrosine phosphorylation and relocation of SHIP are integrin-mediated in thrombin-stimulated human blood platelets. *J. Biol. Chem. 272:26857.*

27. Dyson, J. M., A. D. Munday, A. M. Kong, R. D. Huysmans, M. Matzaris, M. J. Layton, H. H. Nandurkar, M. C. Berndt, and C. A. Mitchell. 2003. SHIP-2 forms tetrameric complex with filamin, actin, and GPIb-IX-V: localization of SHIP-2 to the activated platelet actin cytoskeleton. *Blood 102:940*.

28. Dyson, J. M., C. J. O'Malley, J. Becanovic, A. D. Munday, M. C. Berndt, I. D. Coghill, H. H. Nandurkar, L. M. Ooms, and C. A. Mitchell. 2001. The SH2-containing inositol polyphosphate 5-phosphatase, SHIP-2, binds filamin and regulates submembraneous actin. *J. Cell. Biol. 155:1065*.

29. Daëron, M., C. Bonnerot, S. Latour, and W. H. Fridman. 1992. Murine recombinant FcγRIII, but not FcγRII, trigger serotonin release in rat basophilic leukemia cells. *J. Immunol. 149:1365*.

30. Apgar, J. R. 1990. Antigen-induced cross-linking of the IgE receptor leads to an association with the detergent-insoluble membrane skeleton of rat basophilic leukemia (RBL-2H3) cells. *J Immunol 145:3814*.

31. Aman, M. J., S. F. Walk, M. E. March, H. P. Su, D. J. Carver, and K. S. Ravichandran. 2000. Essential role for the C-terminal noncatalytic region of SHIP in FcγRIIB1-mediated inhibitory signaling. *Mol. Cell. Biol. 20:3576*.

32. Petty, H. R., R. G. Worth, and R. F. Todd, 3rd. 2002. Interactions of integrins with their partner proteins in leukocyte membranes. *Immunol Res 25:75*.

33. Kono, H., T. Suzuki, K. Yamamoto, M. Okada, T. Yamamoto, and Z. Honda. 2002. Spatial raft coalescence represents an initial step in FcγR signaling. *J Immunol 169:193*.

34. Phee, H., W. Rodgers, and K. M. Coggeshall. 2001. Visualization of negative signaling in B cells by quantitative confocal microscopy. *Mol Cell Biol 21:8615*.

35. Monks, C. R., B. A. Freiberg, H. Kupfer, N. Sciaky, and A. Kupfer. 1998. Three-dimensional segregation of supramolecular activation clusters in T cells. *Nature 395:82*.

36. Phee, H., A. Jacob, and K. M. Coggeshall. 2000. Enzymatic activity of the Src homology 2 domain-containing inositol phosphatase is regulated by a plasma membrane location. *J Biol Chem 275:19090*.

Footnotes

Corresponding author: Dr. Marc Daëron, Unité d'Allergologie Moléculaire et Cellulaire, Département d'Immunologie, Institut Pasteur, 25 rue du Docteur Roux, 75015 Paris, France. Tel: (33)1-4568-8642. Fax: (33)1-4061-3160. E-mail: daeron@pasteur.fr

LD-DRM: Low Density-Detergent Resistant Membrane domain

LAT: Linker for activation of T cells

PI3K: Phosphatidylinositol 3-kinase

PLCγ1:Phospholipase C γ-1

PIP3 : Phosphatidylinositol (3,4,5)-trisphosphate

PH : plekstrin homology

BTK : Bruton's tyrosine kinase

BMMC: Bone Marrow-derived Mast Cells

MAR: Mouse anti-rat

TX-100: Triton X-100

PFA: Paraformaldehyde

This work was supported by institutional grants from the Institut National de la Santé et de la Recherche Médicale (INSERM) and the Université Pierre et Marie Curie (Paris VI) and by fellowships from the Ministère de l'Education Nationale et de la Recherche Scientifique and the Association pour la Recherche sur le Cancer (ARC). R.L. is currently the recipient of a fellowship from the Société Française d'Allergologie et d'Immunologie Clinique (SFAIC).

Figure legends

Figure 1. **F-actin disruption decreases FcγRIIB-dependent inhibition of mast cell activation.** (A) Effect of latrunculin B treatment on FcεRI, FcγRIIB and F-actin expression. Cells were incubated with medium or latrunculin B for 18h at 37°C. IgE or 2.4G2 F(ab')$_2$ were added or not in the incubation medium. Aliquots of cells were incubated with IgE or 2.4G2 F(ab)'$_2$ and with FITC-GAM F(ab')$_2$ (to reveal IgE) or FITC-MAR F(ab')$_2$ (to reveal 2.4G2) and fluorescence was analyzed by flow cytometry. Histograms of cells incubated with IgE or 2.4G2 F(ab')$_2$ and FITC-conjugated antibodies were superimposed on histograms of cells incubated with FITC-conjugated antibodies alone. Aliquots of cells were permeabilized, incubated with alexa 488-phalloidin and fluorescence was analyzed by flow cytometry. Histograms of cells incubated with alexa 488-phalloidin were superimposed on histograms of cells incubated with medium alone. (B) Effect of latrunculin B treatment on FcγRIIB-dependent inhibition of mast cell activation. Cells were incubated with the indicated antibodies with or without latrunculin B. FcεRI were then aggregated or coaggregated with FcγRIIB using TNP-MAR F(ab')$_2$. The figure shows the percentages of β-hexosaminidase released in supernatants.

Figure 2. **FcγRIIB and FcεRI translocate into the F-actin skeleton compartment following aggregation or coaggregation.** (A) Western blot analysis of cytosol, membrane and F-actin skeleton subcellular fractions prepared from resting cells. Cytosol, membrane and F-actin skeleton fractions were prepared as described in materials and methods and Western blotted with the indicated antibodies. (B) FcγRIIB redistribution following coaggregation with FcεRI. Cells were incubated with IgE anti-DNP and ^{125}I-2.4G2 F(ab')$_2$ before they were stimulated (+) or not (-) with TNP$_{18}$-MAR F(ab')$_2$. Radioactivity was measured in cytosol,

membrane and F-actin skeleton (F-actin sk.) fractions. The figure shows the percentage of total radioactivity recovered in individual fractions. (C) FcγRIIB redistribution following aggregation. Cells were incubated with ^{125}I-2.4G2 F(ab')$_2$ and with (FcγRIIB/FcεRI coaggregation) or without (FcγRIIB aggregation) IgE anti-DNP. Cells were stimulated or not with TNP$_{18}$-MAR F(ab')$_2$ and cytosol, membrane and F-actin skeleton fractions were prepared. The percentages of radioactivity in the F-actin skeleton fraction were calculated (left panel). Cells expressing intact FcγRIIB or FcγRIIB with a deletion of their intracytoplasmic domains (FcγRIIB-IC$^-$) were incubated with ^{125}I-2.4G2 F(ab')$_2$ and stimulated with TNP$_{18}$-MAR F(ab')$_2$. Cytosol, membrane and F-actin skeleton fractions were prepared and the percentages of radioactivity in the F-actin skeleton fraction were calculated (right panel). (D) Effect of FcγRIIB coaggregation with FcεRI on the translocation of FcεRI into the F-actin skeleton compartment. Cells were incubated with ^{125}I-IgE anti-DNP and with (FcγRIIB/FcεRI coaggregation) or without (FcεRI aggregation) 2.4G2 F(ab')$_2$. Cells were stimulated with TNP$_{18}$-MAR F(ab')$_2$ and cytosol, membrane and F-actin skeleton fractions were prepared. The figure shows the percentages of radioactivity recovered in the F-actin skeleton fraction.

Figure 3. **When coaggregated with FcεRI, FcγRIIB remain excluded from LD-DRM.** (A) Western blot analysis of cell lysates fractionated on sucrose gradient. Unstimulated cells were lysed in 0.06% TX-100-containing lysis buffer. Cell lysates were mixed with a high-density (HD) solution of sucrose, overlaid with two layers of middle- and low-density (MD; LD) solutions of sucrose and ultracentrifuged. Eleven fractions were harvested. Fractions were analyzed by Western blotting with the indicated antibodies. (B) Distribution of FcγRIIB in sucrose gradient fractions following coagregation with FcεRI. Cells were incubated with IgE anti-DNP and ^{125}I-2.4G2 F(ab')$_2$ and stimulated or not with TNP$_{18}$-MAR F(ab')$_2$. Cells were

lysed in 0.06% or 0.1% TX-100-containing lysis buffer and cell lysates were fractionated on gradients as in Fig. 1B. The figure shows the percentage of total radioactivity recovered in individual fractions. (C) Analysis of FcεRI translocation into LD-DRM following aggregation. Cells were sensitized with ^{125}I-IgE anti-DNP and stimulated or not with TNP_{18}-MAR $F(ab')_2$. Cells were lysed in 0.06% or 0.1% TX-100-containing lysis buffer, and cell lysates were fractionated on gradients as in Fig. 1B. The percentages of radioactivity in LD-DRM were calculated.

Figure 4. **The F-actin skeleton compartment contains the high-molecular weight isoform of SHIP1 that interacts with filamin-1 in resting cells.** (A) Distribution of SHIP1 and filamin-1 in subcellular fractions. Fractions were prepared from resting cells as in Fig. 2A, electrophoresed and Western blotted with the indicated antibodies. (B) SHIP1 and filamin-1 cellular localization in resting cells. Cells were permeabilized, stained with Cy5-anti-SHIP1 and FluorX-anti-filamin-1 and examined by confocal microscopy. (C) SHIP1 coprecipitation with filamin-1 in resting cells. Post-nuclear cell lysates were incubated with protein G-coated beads alone or conjugated with either an isotype control or anti-filamin-1 antibodies. Immunoprecipitates were analyzed by Western blotting. (D) Comparative analysis of SHIP1 isoforms that coprecipitated with filamin-1 and with FcγRIIB. Filamin-1 was immunoprecipitated from resting cells as described above. Immunoprecipitates were Western blotted with anti-filamin-1 and anti-SHIP1 antibodies (left panel). FcγRIIB were coaggregated (+) or not (-) with FcεRI and immunoprecipitated. Immunoprecipitates were Western blotted with anti- FcγRIIB and SHIP1 antibodies (right panel). WCL = Whole Cell Lysate.

Figure 5. **Filamin-1 colocalize with SHIP1 and FcγRIIB in small membrane patches following coaggregation with FcεRI.** (A) SHIP1, filamin-1 and F-actin cellular localization

in cells with FcRs patches. Cells were incubated with Cy3-IgE (red) and Cy5-2.4G2 F(ab')$_2$ (blue) and stimulated (lower panel) or not (upper panel) with TNP_{13}-MAR F(ab')$_2$. Cells were fixed, permeabilized, stained with FluorX-anti-SHIP1, FluorX-anti-filamin-1 or alexa 488-phalloidin (green), and examined by confocal microscopy. Arrows show FcR patches. (B) Filamin-1 redistribution in cells presenting small SHIP1 aggregates. FcγRIIB were coaggregated or not with FcεRI, cells were permeabilized and stained with Cy5-anti-SHIP1 and FluorX-anti-filamin-1. Arrows show SHIP1 aggregates.

Figure 6. **Progressive formation of large FcR membrane patches in which SHIP1 remains but from which filamin-1 and F-actin are excluded.** (A) FcR patch size as a function of time following FcγRIIB/FcεRI coaggregation. Cells were incubated with Cy3-IgE and Cy5-2.4G2 F(ab')$_2$ and stimulated or not with TNP_{13}-MAR F(ab')$_2$ for the indicated periods of time. The figure shows the percentage of cells exhibiting one or more than one patch larger than 2 μm. More than 200 cells were analyzed for each time of stimulation. (B) SHIP1, filamin-1 and F-actin cellular localization in cells with large FcRs patches. Cells were treated as indicated in Fig. 6B. White arrows show FcR patches. Red arrows show patches from which filamin-1 or F-actin are excluded. (C) Filamin-1 redistribution in cells presenting large SHIP1 aggregates. Cells were treated as indicated in Fig. 6B. Arrows show SHIP1 aggregates. Red arrows show SHIP1 aggregates from which filamin-1 is excluded. (D) Quantitative analysis of filamin-1 redistribution as a function of the size of FcR patches. FcR patches in which Cy3-IgE and Cy5-2.4G2 F(ab')$_2$ colocalized were measured. Filamin-1 and SHIP1 redistributed with or excluded from FcR patches were examined in individual patches. Each square represents one patch plotted as a function of its size.

Fig. 1

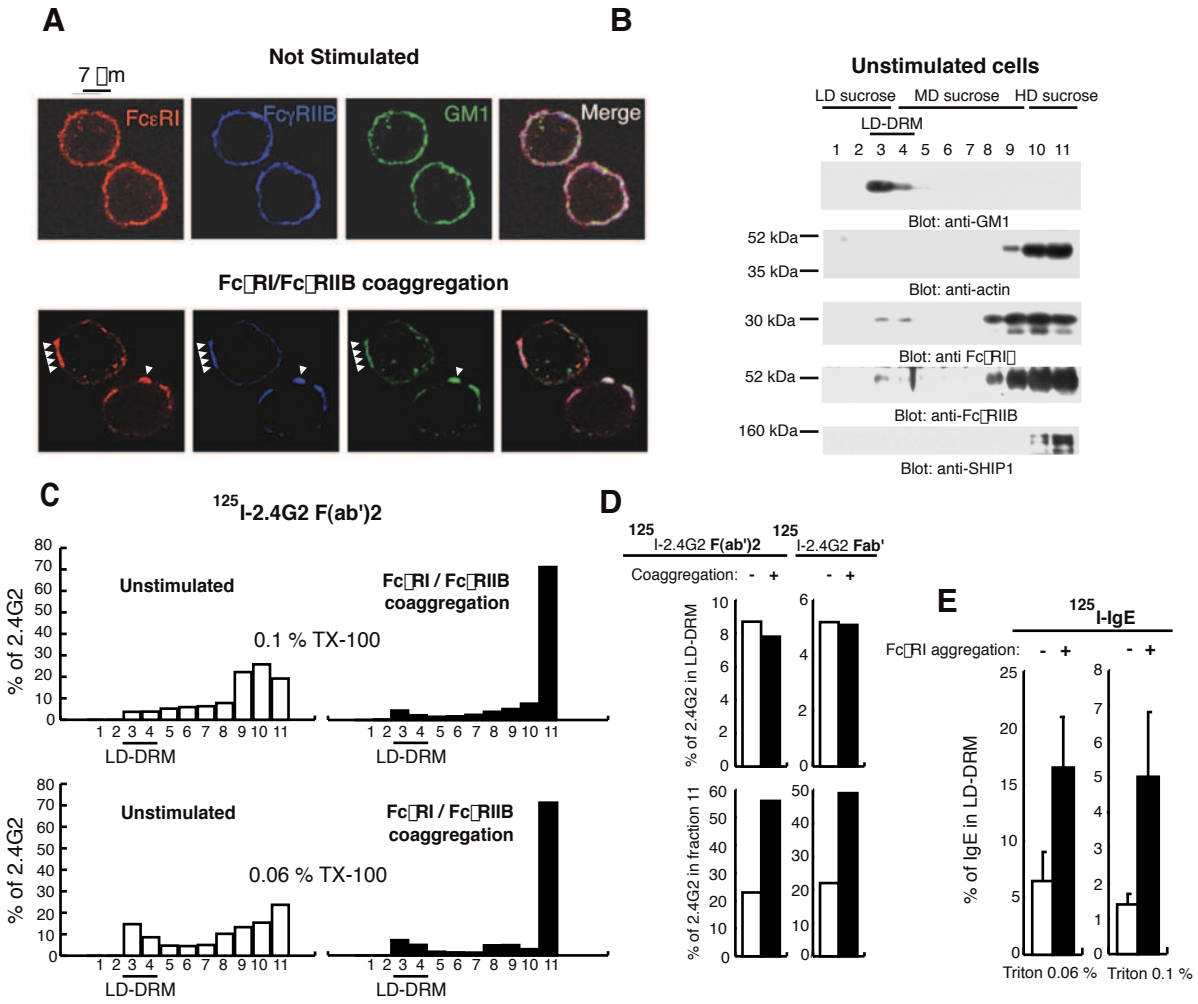

Fig. 2

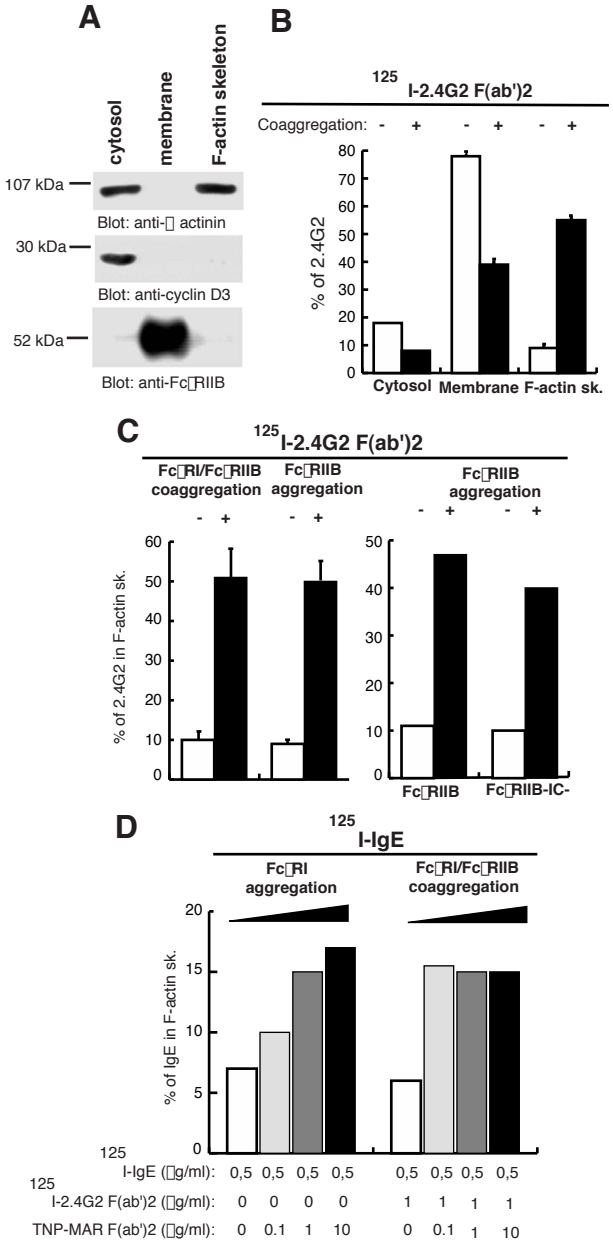

Fig. 3

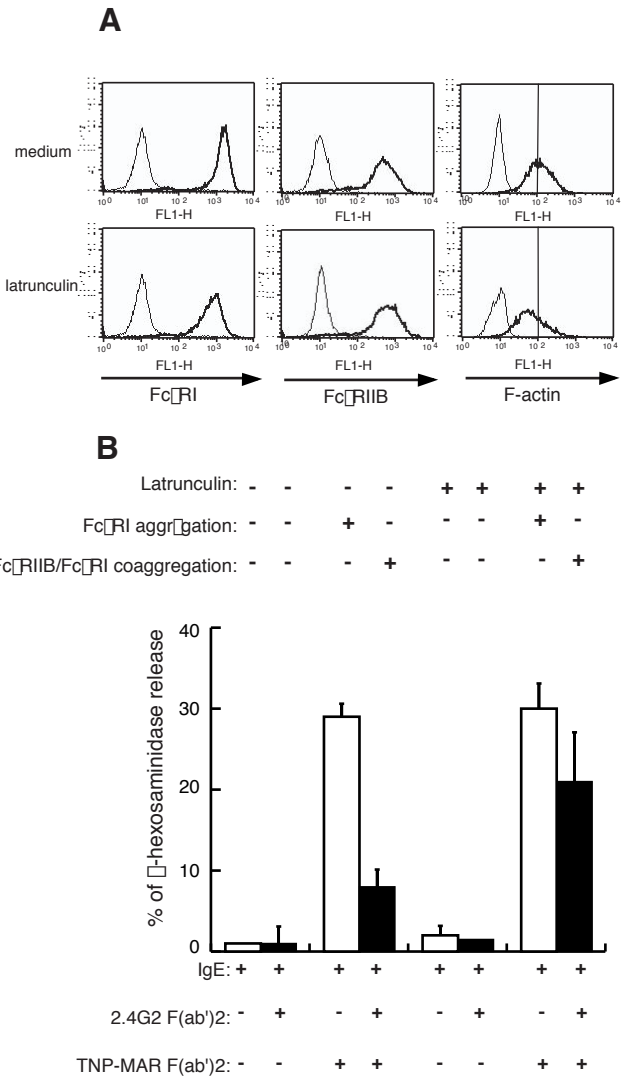

Fig. 4

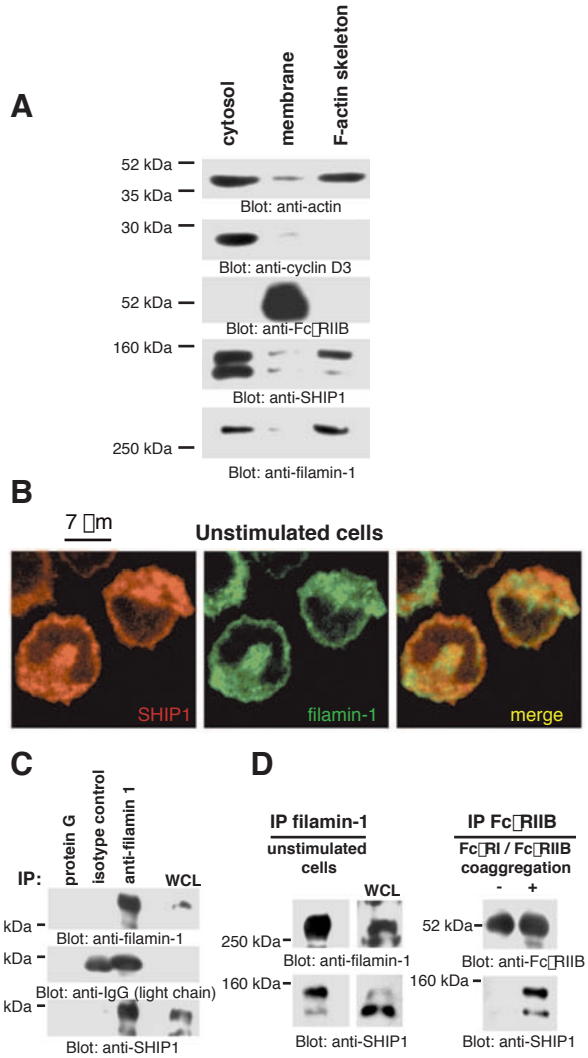

Fig. 5

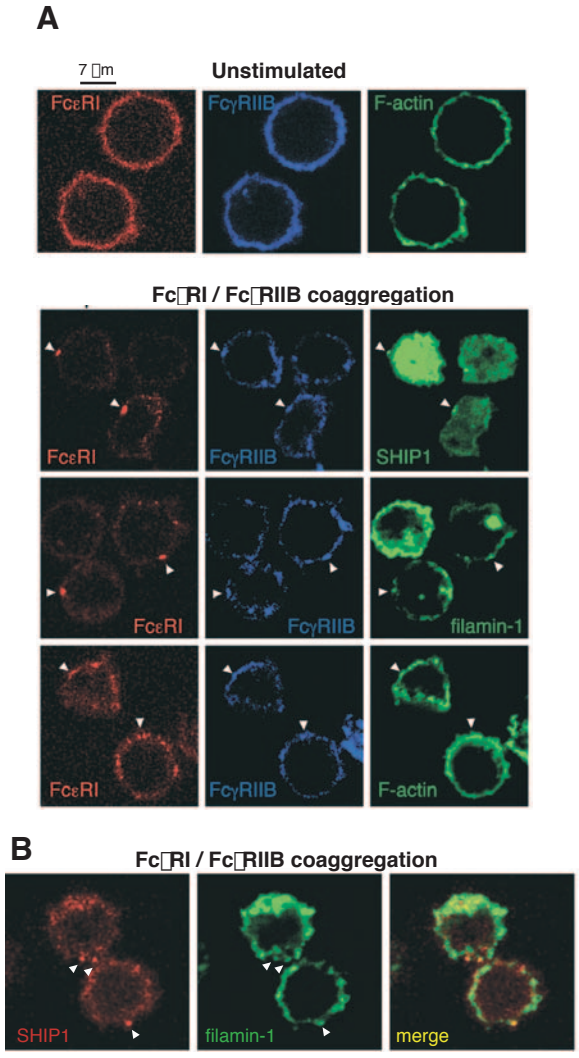

Fig. 6